

This article appeared in a journal published by Elsevier. The attached copy is furnished to the author for internal non-commercial research and education use, including for instruction at the authors institution and sharing with colleagues.

Other uses, including reproduction and distribution, or selling or licensing copies, or posting to personal, institutional or third party websites are prohibited.

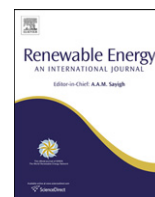
In most cases authors are permitted to post their version of the article (e.g. in Word or Tex form) to their personal website or institutional repository. Authors requiring further information regarding Elsevier's archiving and manuscript policies are encouraged to visit:

<http://www.elsevier.com/copyright>



Contents lists available at ScienceDirect

## Renewable Energy

journal homepage: [www.elsevier.com/locate/renene](http://www.elsevier.com/locate/renene)

# Surface reflectance and conversion efficiency dependence of technologies for mitigating global warming

Ian Edmonds<sup>a,\*</sup>, Geoff Smith<sup>b</sup>

<sup>a</sup> Solartran Pty Ltd., 12 Lentara St, Kenmore, Brisbane 4069, Australia<sup>1</sup>

<sup>b</sup> Physics and Advanced Materials, University of Technology, Sydney, PO Box 123, Broadway, New South Wales 2007, Australia

## ARTICLE INFO

### Article history:

Received 7 December 2009

Accepted 3 November 2010

Available online 3 December 2010

### Keywords:

Global warming

Renewable energy

Geothermal energy

Geo-engineering

Carbon sequestration

Albedo

## ABSTRACT

A means of assessing the relative impact of different renewable energy technologies on global warming has been developed. All power plants emit thermal energy to the atmosphere. Fossil fuel power plants also emit CO<sub>2</sub> which accumulates in the atmosphere and provides an indirect increase in global warming via the greenhouse effect. A fossil fuel power plant may operate for some time before the global warming due to its CO<sub>2</sub> emission exceeds the warming due to its direct heat emission. When a renewable energy power plant is deployed instead of a fossil fuel power plant there may be a significant time delay before the direct global warming effect is less than the combined direct and indirect global warming effect from an equivalent output coal fired plant – the “business as usual” case. Simple expressions are derived to calculate global temperature change as a function of ground reflectance and conversion efficiency for various types of fossil fuelled and renewable energy power plants. These expressions are used to assess the global warming mitigation potential of some proposed Australian renewable energy projects. The application of the expressions is extended to evaluate the deployment in Australia of current and new geo-engineering and carbon sequestration solutions to mitigate global warming. Principal findings are that warming mitigation depends strongly on the solar to electric conversion efficiency of renewable technologies, geo-engineering projects may offer more economic mitigation than renewable energy projects and the mitigation potential of reforestation projects depends strongly on the location of the projects.

© 2010 Elsevier Ltd. All rights reserved.

## 1. Introduction

Governments seek to address global warming by converting from fossil fuel to renewable energy power generation. Implementation of solar power reduces CO<sub>2</sub> emission. However, the accompanying increase in solar absorption and reduction in solar reflection can, initially, increase global warming. Implementation of geo-engineering projects to increase solar reflection can reduce global warming. Therefore, in a situation where additional electrical power is required and global warming is to be minimized within a limited budget it is useful to consider combinations of both approaches. It is only recently that the variation of planet reflectance as a means of mitigating global warming has received attention [1–3]. The variation in local surface reflectance that occurs on deployment of solar power stations or geo-engineering projects results in a variation of the direct local heating at the surface which, in turn, has an effect on global warming, [4]. This paper derives expressions for global temperature change that allow a simple comparison between the different approaches. Variation in radiative forcing [1–4] is usually used to

measure the effect of various technologies on global warming. However, in this paper variation in global temperature is used as the measure as this is more accessible to non-specialists and policy-makers. For similar reasons an accessible greenhouse model capable of analytical solution is used as the basis of the development. Section 2 uses an idealized greenhouse model [5,6] to derive expressions for the change in global temperature with change in the model parameters and relates these to change in local parameters due to different types of power station. Section 3 uses the expressions to find the change in global temperature due to fossil fuelled power stations and renewable energy power stations. Section 4 applies the same approach to current Australian proposals for mitigation via geo-engineering and bio-sequestration so that the mitigation potential can be compared to that of renewable energy technologies. Section 5 introduces two new mitigation strategies. Section 6 is a discussion.

## 2. Idealized greenhouse model

The model used, known as the leaky greenhouse model [5,6], is illustrated in Fig. 1.

One variation to the basic model is the addition of an anthropogenic heat power input,  $P_H$ , delivered at the surface. This leads to

\* Corresponding author. Tel./fax: +61 7 3378 6586.

E-mail address: [ian@solartran.com.au](mailto:ian@solartran.com.au) (I. Edmonds).

<sup>1</sup> [www.solartran.com.au](http://www.solartran.com.au).

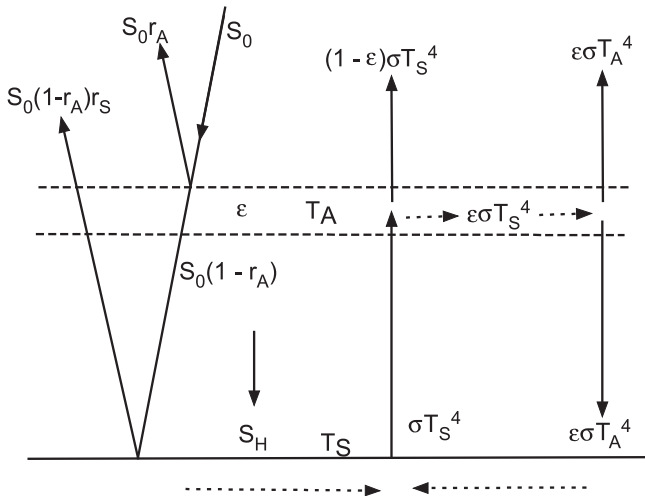


**Fig. 1.** Simple two layer greenhouse model with atmosphere of emissivity,  $\epsilon$ , and surface of emissivity,  $\epsilon = 1$ .

an average heat power flux  $S_H = P_H/4\pi R^2 = P_H/A_E$  at the surface. A second addition is the inclusion of shortwave reflectance at the atmosphere and at the surface. The equilibrium temperatures of the surface and atmosphere are, respectively,  $T_S$  and  $T_A$ .  $S_0$  is the average solar flux,  $342 \text{ W/m}^2$ ,  $A_E$  is the surface area of the Earth ( $A_E = 5.1 \times 10^{14} \text{ m}^2$ ),  $r_A$  is the average atmosphere reflectance,  $r_S$  is the average surface reflectance,  $R$  is the average earth radius,  $6378 \text{ km}$ ,  $\sigma$  is the Stephan Boltzmann constant and  $\epsilon$  is the hemispherical emissivity of the atmosphere.

Zero net energy leaving the planet requires

$$S_0(1 - r_A)(1 - r_S) = \epsilon \sigma T_A^4 + (1 - \epsilon) \sigma T_S^4 \quad (1)$$

Equilibrium at the atmosphere requires

$$\epsilon \sigma T_S^4 = 2\epsilon \sigma T_A^4 \text{ or } T_A^4 = T_S^4/2 \quad (2)$$

Zero energy transfer at the surface requires

$$S_0(1 - r_A)(1 - r_S) + S_H + \epsilon \sigma T_A^4 = \sigma T_S^4 \quad (3)$$

The solution that provides the known surface temperature  $T_S = 288.3 \text{ K}$  and the known planetary absorptance  $(1 - r_A)(1 - r_S) = 0.7$  is obtained with  $\epsilon = 0.78$ . The values  $r_S = 0.15$  and  $r_A = 0.176$  satisfy the product term and are reasonably close to the known atmosphere reflectance and the surface reflectance [7].

By differentiation of equation (3) and use of equations (1) and (2) it can be shown that

$$dT_S/dr_S = -S_0(1 - r_A)T_S/(S_0(1 - r_A)(1 - r_S) + S_H) \quad (4)$$

$$dT_S/dS_H = T_S/(4(S_0(1 - r_A)(1 - r_S) + S_H)) \quad (5)$$

and

$$dT_S/d\epsilon = T_S/8\left(1 - \frac{\epsilon}{2}\right) \quad (6)$$

Substitution of the equilibrium values for  $T_S$ ,  $\epsilon$ ,  $r_S$  and  $r_A$  and with  $S_H = 0$  we obtain

$$dT_S = -85dr_S \text{ K} \quad (7)$$

$$dT_S = 0.3dS_H \text{ Km}^2/\text{W} \quad (8)$$

$$dT_S = 59d\epsilon \text{ K} \quad (9)$$

To a reasonable approximation  $\epsilon = \epsilon_{\text{H}_2\text{O}} + \epsilon_{\text{CH}_4} + \epsilon_{\text{ozone}} + \epsilon_{\text{CO}_2} = \epsilon_0 + \epsilon_{\text{CO}_2}$ . This may be expressed as  $\epsilon = \epsilon_0 + k \ln[C(t)/C(0)]$ , where  $C(t)$  is the mass of  $\text{CO}_2$  in the atmosphere at some time  $t$ ,  $C(0)$  is the mass of  $\text{CO}_2$  in the atmosphere at some reference time usually taken as pre-industrial 1750, and  $k$  is a constant to be determined. Differentiating this expression we obtain  $d\epsilon = k[dC(t)/C(0)]$ . Substitution of this expression for  $d\epsilon$  in equation (9) we obtain  $dT_S = 59k[dC(t)/C(0)]$ . For the case of no feedback mechanisms the IPCC 2007 [8] estimated  $dT_S = 1.2 \text{ K}$  for  $\text{CO}_2$  doubling from the pre-industrial  $\text{CO}_2$  level in the atmosphere, i.e. when  $dC(t) = C(0)$ . Then  $59k = 1.2$  and  $k = 0.0203$ . Thus equation (9) can be written  $dT_S = 1.2 dC(t)/C_{1750}$  and this determines the sensitivity of surface temperature  $T_S$  to changes in  $\text{CO}_2$  content. The current sensitivity with no feedback is  $dT_S = 1.2 dC(t)/C$  where  $C$  is the current  $\text{CO}_2$  content of the atmosphere,  $C = 3000 \text{ Gtonnes}$ . Thus equation (9) may be written as

$$dT_S = 1.2dC/C \text{ K} \quad (10)$$

Feedback occurs when a change in surface temperature due, for example, to an increase in  $\text{CO}_2$  content of the atmosphere induces changes such as greater ocean evaporation and methane emission, and less solar reflecting ice, which result in further change in surface temperature. The overall effects of feedback may be accommodated by including a feedback multiplier,  $F$ , in the equations for  $dT_S$ . Thus the overall temperature change may be written by combining equations (7), (8) and (10) as

$$dT_S = F(1.2[dC/C] + 0.3dS_H - 85dr_S) \text{ K} \quad (11)$$

The current view of the IPCC [8] is that the feedback factor is  $F = 3$  so, in this paper, we use

$$dT_S = 3.6[dC/C] + 0.9dS_H - 255dr_S \text{ K} \quad (12)$$

When comparing global temperature changes due to  $\text{CO}_2$  emission, local heat production and surface reflectance change it is important that any feedback multiplier is applied equally to each mechanism. Equations (11) and (12) ensure this. In this paper we assume that local changes in  $\text{CO}_2$  emission, heat emission and surface reflectance lead to global changes. Thus a local emission of  $\text{CO}_2$  of amount  $dC$  leads to a change  $dC$  in the global  $\text{CO}_2$  content of the atmosphere. Similarly a local power emission  $dP_H$  leads to a change  $dS_H = dP_H/A_E$  in the global surface heat emission and a local variation in surface reflectance ( $r_{S2} - r_{S1}$ ) of an area  $A$  leads to a change in global surface reflectance  $dr_S = (A/A_E)(r_{S2} - r_{S1})$ . Thus equation (12) can be written as

$$dT_S = 3.6[dC/C] + 0.9[dP_H/A_E] - 255(A/A_E)(r_{S2} - r_{S1}) \text{ K} \quad (13)$$

### 3. Global warming on deployment of power stations

This paper seeks to quantify the benefits of implementing different types of renewable energy power stations in place of fossil fuelled power stations. The latter represent the “business as usual” (BAU), method of supplying electrical power. Deployment of a power station results in increased electrical power output  $dP_E$ . If the conversion efficiency is  $e$  the additional heat emission to the atmosphere occurs at a rate  $dP_H = dP_E/e$ . Here the waste heat exhausted in the cooling towers and the heat resulting from end uses of the electrical power are included in  $dP_H$  so that  $dP_H$  is the rate at which heat is produced by burning fuel. The conversion efficiency of fossil fuel power stations varies from about 0.25 for brown coal power stations to about 0.55 for combined cycle gas power stations. In this paper the conversion efficiency of fossil fuelled power stations is taken as  $e = 0.30$ . The change in global heat emission flux can be expressed as

$$dS_H = dP_H/A_E = dP_E/(eA_E) \text{ W/m}^2 \quad (14)$$

To compare equal output power stations it is useful to also express the other two terms in equation (13) in terms of the increase in electrical power output  $dP_E$ . If a coal fired power plant with electrical power output  $dP_E$  operates for  $N$  years the electrical energy delivered is  $NdP_E \times 365 \times 24 \text{ Wh} = NdP_E \times 365 \times 24 / 10^9 \text{ GWh}$ . The production of one GWh of electrical energy from black coal causes the emission of 1000 tonnes of  $\text{CO}_2$ . Thus, after  $N$  years the accumulated  $\text{CO}_2$  emission is

$$\begin{aligned} dC(N) &= NdP_E \times 365 \times 24 \times 1000 / 10^9 \\ &= N(0.00876)dP_E \text{ tonnes } \text{CO}_2 \end{aligned} \quad (15)$$

The emission intensity of 1000 tonnes  $\text{CO}_2/\text{GWh}$  used here represents an average emission intensity for Australian electricity production – primarily from black coal. The carbon intensity varies from about 1400 tonnes  $\text{CO}_2/\text{GWh}$  for brown coal to about 600 tonnes  $\text{CO}_2/\text{GWh}$  for natural gas. Different emission intensities can be accommodated by including an emission intensity factor  $F_{EI}$  in equation (15).  $F_{EI} = 1$  for coal plants and 0.6 for gas fired plants. A further assumption implicit in equation (15) is that the  $\text{CO}_2$  added to the atmosphere remains in the atmosphere indefinitely (infinite lifetime), and that the added  $\text{CO}_2$  and the resultant temperature change increase linearly with time. In fact  $\text{CO}_2$  has a finite residence time in the atmosphere and the level of  $\text{CO}_2$  relaxes towards a new equilibrium level by exchange with the large land and oceanic  $\text{CO}_2$  reservoirs. The relaxation of  $\text{CO}_2$  towards an equilibrium level can be accommodated by replacing  $N$  by the factor  $f(N)$  in equation (15). The value of  $f(N)$  is the integral of the Bern function [3,9] and may be written as

$$\begin{aligned} f(N) &= 0.18N + 0.14 \times 420(1 - \exp(-N/420)) + 0.18 \times 70 \\ &\quad \times (1 - \exp(-N/70)) + 0.24 \times 21(1 - \exp(-N/21)) \\ &\quad + 0.26 \times 3.4(1 - \exp(-N/3.4)) \end{aligned}$$

Including  $F_{EI}$  and  $f(N)$  equation (15) becomes

$$dC(N) = f(N)F_{EI}(0.00876)dP_E \text{ tonnes } \text{CO}_2 \quad (17)$$

When a solar power plant is deployed the average electrical output is given by  $dP_E = (1 - r_A)S_0Ae_S$  where  $A$  is the area of the collector,  $r_A$  is the reflectance of the atmosphere and  $e_S$  is the solar to electric power conversion efficiency. Thus the required area of collector may be expressed in terms of the electrical output as  $A = dP_E / ((1 - r_A)S_0e_S)$ . If the collector has reflectance  $r_{SC}$  and the collector is deployed on ground of ground reflectance  $r_{SG}$  the change in global surface reflectance is  $dr_S = (A/A_E)(r_{SC} - r_{SG}) = dP_E(r_{SC} - r_{SG}) / (S_0(1 - r_A)A_Ee_S)$ . Including this expression and equations (14) and (17) in equation (13) we obtain the overall change in global temperature

$$\begin{aligned} dT_S &= [3.6 f(N)F_{EI}(0.00876)/C + 0.9/eA_E - 255(r_{SC} - r_{SG}) / \\ &\quad \times (S_0(1 - r_A)A_Ee_S)]dP_E \end{aligned}$$

which with  $r_A = 0.176$ ,  $C = 3 \times 10^{12}$  tonnes and  $A_E = 5.1 \times 10^{14} \text{ m}^2$  becomes

$$dT_S = [10f(N)F_{EI} + 1.8/e - 1.8(r_{SC} - r_{SG})/e_S]10^{-15}dP_E \text{ K} \quad (18)$$

This equation allows a simple comparison of the global warming of fossil fuelled and solar power stations of equal average power output,  $dP_E$ . The numeric constants have been rounded to two significant digits since accuracy is generally lower than 1%. We consider:

- (1) Coal fired,  $e = 0.3$ ,  $F_{EI} = 1$ .
- (2) Gas fired,  $e = 0.3$ ,  $F_{EI} = 0.6$



Fig. 2. Kramer junction type concentrating solar thermal power station [10].

- (3) Concentrating solar thermal, Kramer Junction type, Fig. 2,  $e_S = 0.14$ , collector reflectance  $r_{SC} = 0.15$ , ground reflectance  $r_{SG} = 0.35$  [10].
- (4) Flat plate photovoltaic,  $e_S = 0.1$ ,  $r_{SC} = 0.1$ ,  $r_{SG} = 0.35$ .
- (5) Solar chimney plant, Fig. 3,  $e_S = 0.005$ ,  $r_{SC} = 0.25$ ,  $r_{SG} = 0.35$  [11].
- (6) Biomass power plant  $e_S = 0.001$ ,  $r_{SC} = 0.2$ ,  $r_{SG} = 0.35$ .
- (7) Geothermal power plant  $e = 0.1$  [12].

For comparison purposes the average electrical power output,  $dP_E$ , of each power station is taken as 1 GW. For a fossil fuelled power plant the first two terms in equation (18) are used. For a nuclear or geothermal power plant only the second term is used. For a solar powered plant only the last term is used. The ground reflectance  $r_{SG}$  is taken as the reflectance of dry desert  $r_{SG} = 0.35$  [13,14]. The collector reflectance,  $r_{SC}$ , of the solar chimney plant is taken as the reflectance of the grass, 0.25, that covers the ground below the collector glazing. The solar conversion efficiency of the biomass power plant,  $e_S = 0.001$ , is taken as the product of the solar energy to biomass energy conversion efficiency, 0.3%, [15], and the thermal efficiency of a biomass fuelled power station, 33%. The global temperature change in microKelvin during 100 years after implementation of 1 GW of each of the seven types of power station is shown in Fig. 4.

The coal and gas fuelled plants show a small initial step in temperature due to heat emission followed by an increase due to the accumulation of  $\text{CO}_2$  in the atmosphere. The geothermal power

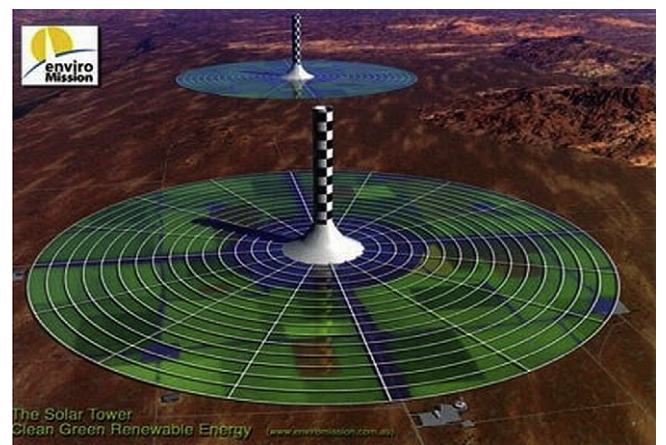


Fig. 3. Conceptual diagram of a solar updraft tower and collector [11].



plant shows a moderate step increase in temperature due to heat emission. The solar powered plants show an initial step increase in global temperature due to the change in surface reflectance. This is relatively small for the higher efficiency plants and relatively large for the lower efficiency plants. Evidently, if a solar powered plant is implemented in place of a fossil fuelled plant there will be some finite time before mitigation of global warming becomes effective i.e. some finite time before the warming due to decreased surface reflectance on implementation of a solar power plant falls below the warming that would occur with a similar output fossil fuel power plant. This time can be significant for low efficiency solar power plants. For example the time delay is 43 years if a biomass powered plant replaces a coal fired plant. The step increase in global warming on implementation of a solar powered plant is proportional to  $(r_{SC} - r_{SG})/e_S$  or equivalently  $A(r_{SC} - r_{SG})$ . Thus location of low efficiency solar power plants on locations where  $r_{SG}$  is low and approaches  $r_{SC}$  is useful in reducing global warming. From Fig. 4 the global warming mitigation achieved 50 years after implementing a 1 GW solar thermal or photovoltaic power station in place of a coal fired power station is about 300  $\mu$ K. Smaller implementations provide proportionally smaller mitigations. For example a 1 kW peak residential PV installation provides 0.25 kW average power output and, after 50 years, a warming mitigation of  $300 \times 10^{-6} \times 0.25/10^6 = 75 \times 10^{-12}$  K.

#### 4. Application to geo-engineering and carbon sequestration

Geo-engineering involves altering the planetary reflectance to bring about a change in global temperature [1,3]. In this paper we are concerned with the alteration of global surface reflectance  $r_S$  by changing the reflectance of an area  $A$  of the Earth's surface from  $r_{S1}$  to  $r_{S2}$ . From equation (12) the change in global surface temperature is  $dT_S = -255dr_S = -255(A/A_E)(r_{S2} - r_{S1})$ . When comparing power station projects with geo-engineering projects it is convenient to add this expression as a fourth term to equation (18). Thus equation (18), with the constants to two significant digits, becomes

$$dT_S = (10f(N)F_{EI} + 1.8/e - 1.8(r_{SC} - r_{SG})/e_S)10^{-15}dP_E - 250(A/A_E)(r_{S2} - r_{S1}) K \quad (19)$$

We first compare a \$1 B solar power station project with a \$1 B geo-engineering project. Secondly we assess the effectiveness of projects to sequester CO<sub>2</sub> in forests.

##### 4.1. Comparison of geo-engineering and solar PV

The Google Earth image in Fig. 5 shows a 10,000 km<sup>2</sup> area of Australia that exhibits ground reflectance,  $r_{SG}$ , that varies from about 0.2 in parts of the weathered rock terrain of the Flinders Range to about 0.7 on the white salt flats of Lake Frome. The area is about 450 km North of Adelaide and is indicative of the range of ground reflectance available for the installation of renewable energy power stations in Australia.

The Federal Government Clean Energy Initiative Solar Flagship program [16] will provide funding of about \$1.6 Billion for the construction of solar power stations for a total of 1 GW peak electrical output. A photovoltaic power plant costs about \$5 per peak Watt to deploy or about \$500/m<sup>2</sup>. Thus a \$1.0 B investment would provide a 200 MW peak power plant and the collectors would cover an area  $A = 2 \times 10^6$  m<sup>2</sup> (1.4 km  $\times$  1.4 km), the area of the red square in Fig. 5. With a 1 to 4 ratio between peak and average isolation the average electrical output would be 50 MW and this photovoltaic power station could replace 50 MW of fossil fuelled power. The question arises: When the effect of ground reflectance is taken into account are there more economically beneficial ways of achieving equivalent mitigation in programs similar to the Flagship Program than solar thermal or photovoltaic power plants?

Increasing the reflectance of a surface area can result in an immediate reduction in global temperature as more of the solar energy incident on the area is reflected back to space. White agricultural plastic sheet with high UV resistance and high solar reflectance after weathering ( $r_{SP} = 0.6$ ) is available for about \$1/m<sup>2</sup>. Similarly aluminum coated plastic fabric of the type used for reflective insulation in buildings ( $r_{SAL} = 0.9$ ) is available for about \$1/m<sup>2</sup>. As the PV plant costs about \$500/m<sup>2</sup> the figure \$1/m<sup>2</sup> suggests a white plastic or aluminized reflective surface 500 times larger than the PV collector could be deployed for the same cost.

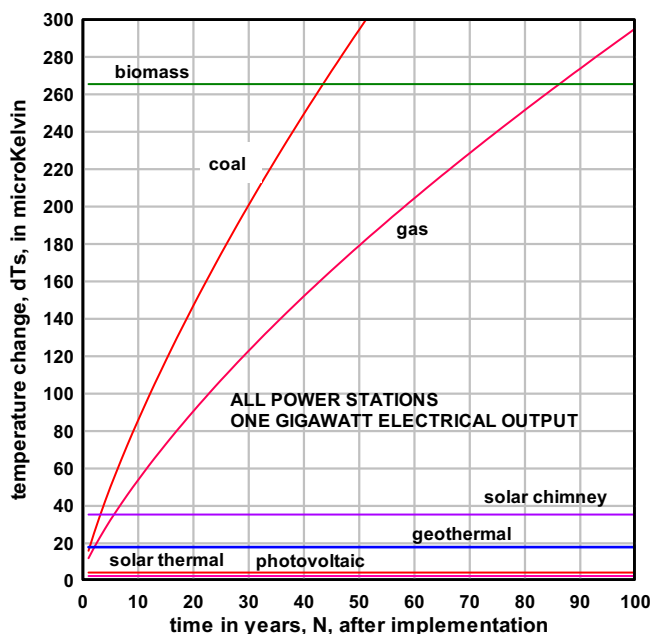


Fig. 4. Global temperature change due to the operation of fossil fuelled or renewable energy power stations each of average electrical output of 1 GW.



Fig. 5. The Flinders Range area of Australia to the left with the Lake Frome salt flats to the right is shown. The ground reflectance,  $r_G$ , varies from about 0.7 on the salt lake to about 0.2 in the ranges.

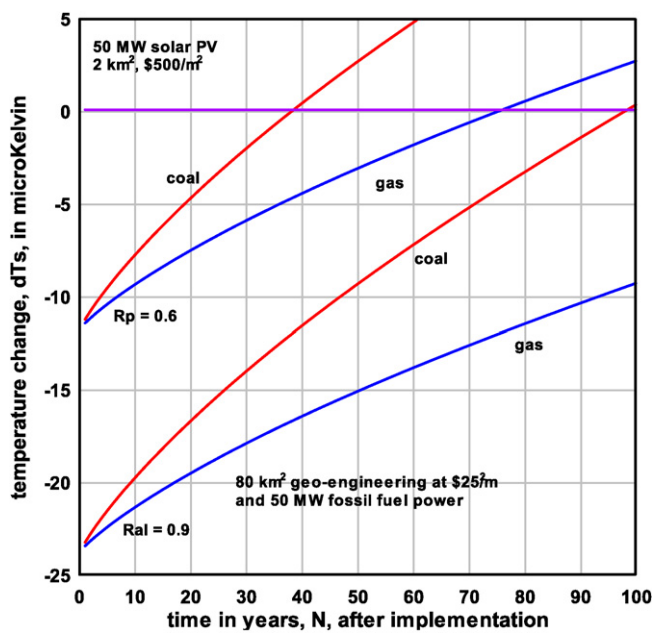


Fig. 6. The global temperature change due to implementation of two \$1 B projects was compared. (1) A 50 MW average PV power station. (2) A geo-engineering project to increase surface reflectance and a 50 MW of fossil fuelled power station.

However, taking into account that some basic support frame would be required a cost of \$25/m<sup>2</sup> for support frame plus reflective material is more realistic. At a cost of \$25/m<sup>2</sup> a \$1 B project would provide a reflective area 40 times larger than the PV collector i.e.  $A = 80 \times 10^6 \text{ m}^2$  (8.9 km  $\times$  8.9 km), the size of the white square in Fig. 5. Therefore a realistic comparison can be made between the supply of 50 MW power by, (1), a 2 km<sup>2</sup>, 50 MW average, PV plant of conversion efficiency  $\epsilon_s = 0.15$  costing \$1 B and, (2), an 80 km<sup>2</sup> geo-engineered reflector located on ground of reflectance  $r_{SG} = 0.3$  costing \$1 B in combination with a conventional 50 MW fossil fuelled power station costing \$2/W or \$0.1 B, i.e. a total cost of \$1.1 B. Other items in a detailed cost estimate would include the lifetime of the reflective material relative to the lifetime of the PV panels, the absence of electric connectors and power transmission in the case of the geo-engineered solution, the availability of areas of low reflectance in Australia and whether Carbon Credits were available for projects that reduce global warming without reducing CO<sub>2</sub> emissions. By using the third term in equation (19) for  $dT_s$  due to the PV plant and the first, second and fourth terms in equation (19) for the geo-engineered reflector plus a conventional fossil fuelled plant we can compare the resulting changes in global temperature. The result is shown in Fig. 6.

Fig. 6 shows that an immediate global cooling is provided on implementation of the projects to increase surface reflectance. In the case of the aluminum reflective material the mitigation of global warming exceeds that obtained by implementing a solar PV station for 100 years. A more detailed analysis would take into account relative lifetimes of the PV panels and the aluminum reflectors as well as the cost of power transmission and losses in transmission in the case of the PV power station. It is interesting to note that an aluminized reflector in space, about  $\frac{1}{4}$  the size (20 km<sup>2</sup>), would produce the same cooling. However, the deployment cost would probably exceed \$1 B.

A similar approach can be applied to assess the Australian State and Federal government schemes to rebate about one half, \$8000, of the cost, \$15,000, of installing one kW peak PV systems on residences. A \$1 B dollar project provides for installations on 125,000 homes and a 125 MW peak PV power supply. With a 4 to 1 ratio

between peak and average isolation this corresponds to a 31.2 MW average power output. An alternative geo-engineering option is to rebate the cost of converting dark roofs to light roofs. The cost of painting a roof is about \$20/m<sup>2</sup> and the average Australian home roof area is about 100 m<sup>2</sup>. Thus the cost per roof is \$2000. In a \$1 B project 500,000 roofs of total area 50 km<sup>2</sup> could be geo-engineered. The average solar reflectance of the four darker roof colors in the Colorbond steel roofing range commonly used on Australian roofs is 0.26. The reflectance of the lightest color in the Colorbond range is 0.69. This suggests a change in average solar reflectance of 0.43 could be achieved if darker roofs were targeted in the project. Using equation (19) as before a comparison of global temperature change can be made between, (1), residential PV installed on 125,000 homes producing 31.2 MW average for a cost of \$1 B and (2), a dark to light roofs program targeting 500,000 homes costing \$1 B plus conventional fossil fuelled power of 31.2 MW costing \$ 0.06 B for a total cost of \$ 1.06 B. The result is shown in Fig. 7.

Fig. 7 shows that a dark to light roofs project would provide an immediate mitigation of global warming that is not exceeded by the PV project until 60 years have elapsed – much longer in the case where the 31 MW of fossil power is gas fuelled. A more detailed analysis would take account of the lifetime and the maintenance costs of PV panels relative to painted roofs.

#### 4.2. Carbon sequestration

As an example of a typical Australian carbon sequestration project a large Australian energy company announced recently [17] a project to plant Mallee eucalypt trees in the marginal wheat-belt regions of Australia to generate carbon credits tradable under the government's Carbon Pollution Reduction Scheme. The full project of 30 million trees would sequester about 6 millions tonnes of carbon. The combined climate and carbon-cycle effects of large scale forest projects have been studied using three-dimensional climate models [18–20]. The results of these studies indicate that the mitigation potential of reforestation projects is strongly latitude

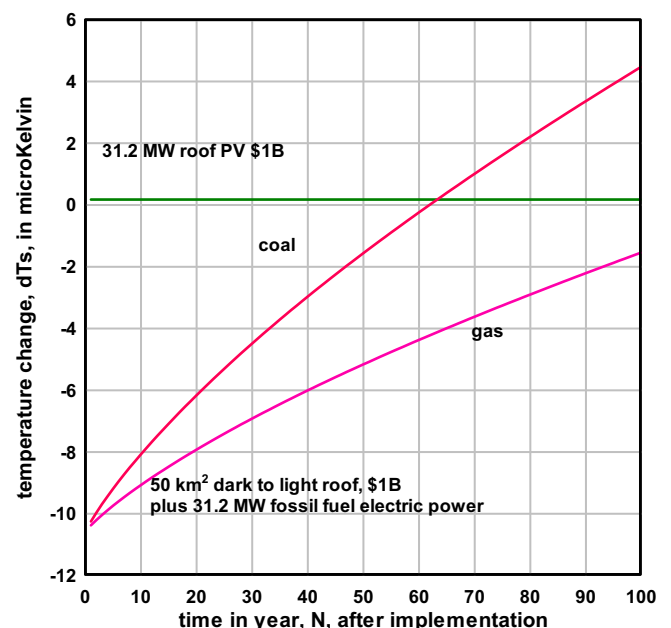


Fig. 7. The global temperature change due to implementation of alternative \$1 B projects was compared. (1) A 31 MW average PV power project involving installing one kW peak supplies on 125,000 residences. (2) A project that converts 500,000 dark residential roofs to a lighter color by painting plus 31 MW of fossil fuelled power.

and terrain dependent with projects at higher latitudes much less effective than reforestation in the tropics. These models are not readily accessible to researchers. However, much insight into the effects of reforestation can be gained from application of the simple equations developed in this paper.

Fig. 8 shows part of the wheat-belt area south east of Lake Grace in Western Australia. The square forested area evident in Fig. 10 (Lake Magenta National Park) covers an area of 730 km<sup>2</sup>. Assuming this area contains mature forest the accumulated carbon sequestration is about 120 tonnes per acre for pine forest and about 40 tonnes per acre for dry hardwood forest [21]. Conversion of the lower (dry hardwood) figure to CO<sub>2</sub> sequestration yields a figure of 33,000 tonnes CO<sub>2</sub>/km<sup>2</sup>. In this case the total amount of CO<sub>2</sub> sequestered in the 730 km<sup>2</sup> area is  $dC = 24$  million tonnes. In the case of pine forest the amount sequestered would be 72 million tonnes.

Now consider the implementation of a carbon sequestration project where dry wheat-belt farmland of the same area as the Magenta National Park (730 km<sup>2</sup>) is converted to forest. Growing forest on the wheat-belt area decreases the ground reflectance from about 0.3 to about 0.1. Of the solar power absorbed by the forest less than 2% is converted by photosynthesis into plant matter. Nearly all of the absorbed power is dissipated as heat into the atmosphere by convection and by evaporation of water via plant respiration. Therefore not all of the absorbed energy is radiated by the forest to the atmosphere. However, ultimately all the absorbed energy enters the radiation exchange between the global surface and the global atmosphere and the equations derived here are applicable. The global temperature rise can be found from the third term in equation (13),  $dT_s = -255(A/A_E)(0.1-0.3) = 73 \mu K$ . This can be compared with the global temperature decrease due to the sequestration of CO<sub>2</sub> in the forest. We assume that within a few years the ground is covered with young trees and that the sequestration of CO<sub>2</sub> in the trees increases steadily to maturity at 50 years. Thus in the case of hardwood forest the increase in CO<sub>2</sub> sequestration after  $N$  years is given by  $dC_F(N) = (24/50)N = 0.48N$  million tonnes CO<sub>2</sub> and for the case of pine forest  $dC_F(N) = 1.44N$  million tonnes CO<sub>2</sub>. However, the resulting decrease in CO<sub>2</sub> content of the atmosphere will be lower due to the finite lifetime of perturbations of atmospheric CO<sub>2</sub> due to exchange with the large CO<sub>2</sub> reservoirs. Thus  $dC(N) = -f(N)dC_F(N)$  where  $f(N)$  is the decay

factor of equation (16). Using equation (13) to compare the temperature changes we obtain the result in Fig. 9.

From Fig. 9 we see that on establishment of a young forest of reflectance  $r_{SF} = 0.1$  on 730 km<sup>2</sup> of dry wheat land of reflectance  $r_{SW} = 0.3$  there is a global temperature increase of 73  $\mu K$ . As the trees grow towards maturity at 50 years there is a decrease in global temperature as CO<sub>2</sub> is sequestered in the maturing trees. In the example of Fig. 9 the end result of establishment of mature forests after 50 years is still a net warming. However, this result is strongly dependent on the values of land reflectance and forest reflectance used in the calculation. Wheat land reflectance varies strongly with season [22] and this should be taken into account in a detailed analysis. However, at the time the image in Fig. 8 was made the reflectance of the forest area was significantly lower than the reflectance of the wheat land. An approximate estimate of ground reflectance can be found from Google Earth images such as Fig. 8 provided the image contains a water reservoir (reflectance 0.05) and a salt flat (reflectance 0.6) that can be used as a reference for photometric measurement from the screen image. This is useful when assessment of reflectance on a continental scale is required. However, it provides approximate reflectance only and at only one instant of time.

The above analysis indicates that the current Australian schemes to obtain Carbon Credits by reforesting areas of dry wheat-belt land could be effective in reducing the amount of CO<sub>2</sub> in the atmosphere and reducing global warming provided the reforestation project is located on ground of low solar reflectance. Areas in the Flinders Range, Fig. 6, would be ideal as is any area with existing scrub vegetation. If such locations were selected for reforestation projects areas of about 1000 km<sup>2</sup> could achieve global cooling of about 100  $\mu K$  on maturity in 50 years. To achieve a mitigation of 0.1 K (10,000  $\mu K$ ) an area of 100,000 km<sup>2</sup> would be required, which is about 1% the total area of Australia (7,700,000 km<sup>2</sup>).

## 5. New mitigation strategies

The equations developed here allow the comparison of new warming mitigation strategies against existing strategies. This

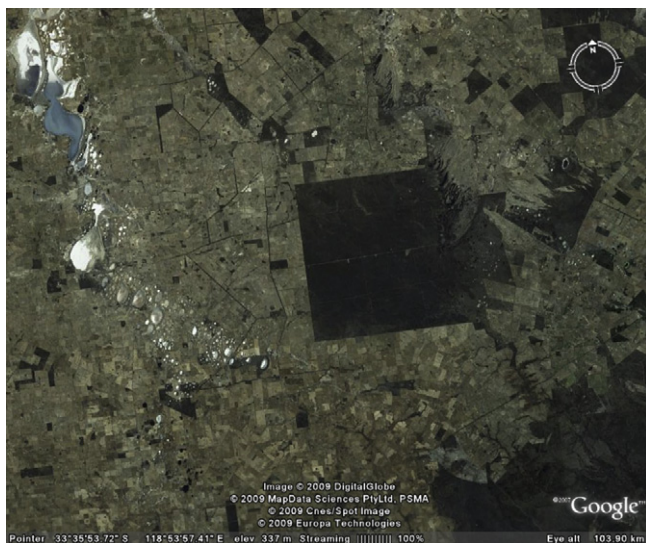


Fig. 8. The 730 km<sup>2</sup> square area of forest in the West Australian wheat land would sequester 24 million tonnes CO<sub>2</sub> if hardwood forest and 72 million tonnes CO<sub>2</sub> if pine forest.

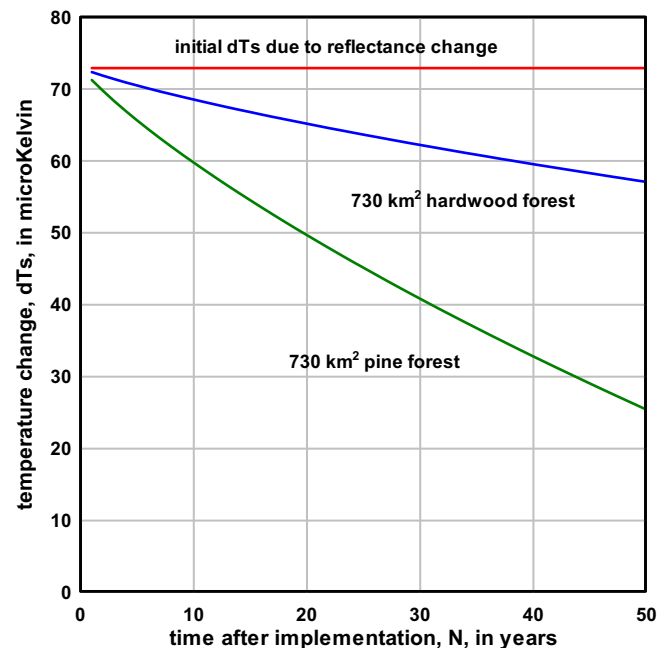


Fig. 9. The variation of global temperature on establishment of a forest to sequester CO<sub>2</sub> from the atmosphere. It is assumed that sequestration in the forest increases linearly with time up to maturity at  $N = 50$  years.



section introduces strategies for: (1), mitigation of warming and salinity and (2), mitigation of warming and drought. The strategies are especially appropriate in Australia as salinity and drought are perennial problems. Each mitigation strategy is compared with the mitigation potential of the more conventional options discussed in Section 3.

### 5.1. Mitigation of warming and salinity

A low cost approach to geo-engineering ground reflectance, with ancillary agricultural benefits, is to convert land currently degraded or threatened by rising salty groundwater to an admix of salt pans and reclaimed land. This is done by pumping salty groundwater into shallow evaporation basins while the falling water table on the remaining farmland returns it to higher yields. Vast tracts of Australian farmland are threatened by rising water tables. When native vegetation is replaced by crops or pasture rain water passes beyond the root zone and the water table begins to rise – between 12 and 35 mm per annum in the dryer farmland zone [22]. A salinity mitigation strategy is to pump saline groundwater into evaporation basins to lower the water table. This also forms a salt pan with much higher reflectance than the surrounding farmland. The result is an immediate mitigation in global warming. As an example the image in Fig. 10 is a 700 m × 900 m (63 ha) wheat field in which a 66 m diameter evaporation basin has been established.

The area of the basin is  $3.4 \times 10^3 \text{ m}^2$  and the basin evaporation rate in this area is 2 m/year [23]. Thus the basin evaporates  $6.8 \times 10^3 \text{ m}^3$  of water per year. To supply this water from the water table requires a pumping rate of 6.8 ML/year or 19 kL/day over a head of about 2 m. The pump power required is about 40 W. This pumping lowers the water table in the field by  $6.8 \times 10^3 / 63 \times 10^4 = 0.011 \text{ m}$  or 11 mm per year which is a significant mitigation of the water table rise. When the ground reflectance changes from 0.2 to 0.6 on establishment of the basin the immediate global warming mitigation is  $dT_s = -255(A/A_E)(r_{S2} - r_{S1}) = -0.68 \times 10^{-9} \text{ K} = -0.00068 \mu\text{K}$ . This is about 10 times higher than the mitigation achieved after 50 years operation when 1 kW of PV power replaces 1 kW of fossil power in residential power supply ( $\Delta T(50) = 0.075 \times 10^{-9} \text{ K}$ , Section 3). Government currently supports installation of 1 kW peak residential

PV with an \$8000 subsidy. This analysis suggests a similar subsidy of \$8000 for the establishment of evaporation basins similar to Fig. 10 on saline effected farmland would provide an immediate global warming mitigation about ten times greater than that achieved by the \$8000 subsidy for residential PV. Alternatively, if farmers were paid for the equivalent CO<sub>2</sub> offsets in Carbon Credits, and also gained from the remediated land, this would be a very cost effective approach to global warming mitigation.

### 5.2. Mitigation of warming and drought

An approach to geo-engineering ground reflectance, with ancillary water conservation benefits, is to install reflective evaporation mitigation covers on the highly absorbing surface of water reservoirs. The Wivenhoe, Somerset and North Pine dams that supply South East Queensland (SEQ) with water have a total area of 170 km<sup>2</sup>. The pan evaporation rate in SEQ is 2 m/year [23] thus the evaporation rate from the dams is 340 GL/year. The current water consumption in SEQ is 340 GL/year [24]. Thus the dams lose by evaporation as much as the residents consume. Evaporation mitigation systems [25], similar to the example shown in Fig. 11, are up to 90% efficient in reducing evaporation so that an additional  $340 \times 0.9 = 306 \text{ GL/year}$  can be made available for consumption by implementing evaporation mitigation systems on the dams. Residential consumption is expected to increase to 760 GL/year by 2040. Clearly evaporation mitigation could supply most of this increase. The Queensland government currently envisages meeting supply with three new desalination plants (182 GL/year) and a new dam and by raising the level of existing dams (140 GL/year), a total investment of about \$3 B [26]. The cost of deploying an evaporation mitigation system as in Fig. 11 was estimated to be \$20/m<sup>2</sup> in 2005 [27]. The total cost of implementation for all three dams would be  $170 \times 10^6 \times 20 = \$3.4 \text{ B}$ . Thus the cost of desalination plants and new and raised dams (\$3 B) is about the same as the cost of an evaporation mitigation cover. However, an evaporation mitigation cover can also mitigate global warming.

Evaporation mitigation systems as in Fig. 11 convert dam surface reflectance from 0.1 to 0.6 and therefore provide a large and immediate global warming mitigation in addition to the evaporation mitigation. Implementing covers on all of the 170 km<sup>2</sup> dam surface would result in an immediate temperature change  $dT_s = -255(A/A_E)(0.6 - 0.1) = -42 \mu\text{K}$ . Referring to Fig. 4 a temperature change of  $-42 \mu\text{K}$  would offset the warming produced after 4 years operation of a 1 GW coal fired power station. From equation (15) four years operation of a 1 GW power station emits 35 million tonnes of CO<sub>2</sub>. If geo-engineering projects attracted Carbon Credits under an emission trading scheme (ETS) for temperature mitigation equivalent to CO<sub>2</sub> mitigation this project



Fig. 10. Image of a 700 m × 900 m wheat field in Western Australia in which a 66 m diameter evaporation pond has been established.



Fig. 11. Reflective evaporation covers on a mine reservoir at Parkes, NSW, Australia.



would attract Carbon Credit for 35 million tonnes CO<sub>2</sub> equivalence. The projected price for Carbon Credits under the Australian ETS is \$40/tonne CO<sub>2</sub>. Thus this project could attract \$1.4 B in Carbon Credits reducing the implementation cost to \$2 B, substantially lower than the cost of the alternative water supply scheme (\$3.4 B). A more detailed analysis would take account of the lifetime of evaporation mitigation covers and the CO<sub>2</sub> emissions from operation of the three desalination plants.

## 6. Discussion

The equations derived in this paper apply only to power plants that generate electricity by converting thermal energy or radiant energy to electricity. The expressions are not relevant to renewable technologies such as wind turbines or tidal turbines that convert mechanical energy to electricity. The equations take into account the direct heat emission and the displaced CO<sub>2</sub> emission in assessing the climate change impact of renewable energy technologies. The direct heat emission includes heat produced by burning coal, the heat produced by extraction of geothermal energy and the heat produced when a solar energy collector changes the surface reflectance at the site where it is deployed. The equations provide a simple means for comparing the effectiveness of different renewable energy technologies in mitigating global warming relative to coal or gas based power (“BAU” case). The measures of effectiveness provided are the delay in years before the deployment of a particular technology results in a mitigation of global warming relative to “BAU” and the temperature mitigation achieved N years after deployment. These equations indicate that for efficient renewable energy technologies such as concentrating solar power stations the time delay before mitigation of warming becomes effective is small or zero. A significant instant benefit is possible in most cases. For technologies with very low conversion efficiency the time delay before mitigation becomes effective may be significant. The examples outlined show that the warming mitigation potential of technologies to reduce global warming can be sensitive to the ground reflectance of the locality where the technology is deployed. Low efficiency solar technologies should be deployed in areas of low reflectance to maximize the potential for mitigation. The approach used here is also useful in establishing the effectiveness of geo-engineering and bio-sequestration methods for mitigating global warming. In particular it is shown that deployment of geo-engineering solutions in desert areas of Australia may be as cost effective in mitigating global warming as the deployment of PV or solar thermal power plants. In the case of bio-sequestration or reforestation projects the approach used here indicates that the warming mitigation potential of Australian reforestation projects depends quite strongly on the ground reflectance where the projects are implemented.

## 7. Conclusion

This work quantified the delay before the direct temperature increase on implementing renewable energy generators is compensated by the temperature mitigation due to the offset of fossil fuel power generation. For low conversion efficiency renewable technologies the delay can be substantial e.g. years for geothermal power and decades for biomass power. Also quantified was the delay, several decades, before the immediate mitigation available from a combination of surface geo-engineering and fossil fuelled power is exceeded by the mitigation available from renewable energy power. This work also demonstrated that there are water supply options based on geo-engineering reservoirs that provide immediate mitigation of warming and could be more cost effective than options such as desalination which increase global warming. In view of the possibility that near zero emission

technologies such as nuclear and carbon capture power may be available in Australia within a few decades these findings should influence policy directions with respect to global warming.

## Nomenclature

A	area of collector (m <sup>2</sup> )
A <sub>E</sub>	Earth surface area ( $5 \times 10^{14}$ m <sup>2</sup> )
C	current mass of atmospheric CO <sub>2</sub> (3000 Gtonnes)
C <sub>F</sub>	carbon dioxide sequestered in a forest (tonnes)
C(t)	mass of carbon dioxide in the atmosphere at time t (tonnes)
C <sub>1750</sub>	mass of pre-industrial atmospheric CO <sub>2</sub> (tonnes)
e	heat to electrical power conversion efficiency
F <sub>EI</sub>	emission intensity factor (F <sub>EI</sub> = 1 for coal, 0.6 for gas)
f(N)	fraction of CO <sub>2</sub> change remaining after N years (Bern function)
k	constant relating CO <sub>2</sub> and atmosphere emissivity
N	number of years
P <sub>E</sub>	electrical power output (W)
P <sub>H</sub>	anthropogenic heat power at the surface (W)
R	Earth radius (m)
r <sub>A</sub>	reflectance of the atmosphere
r <sub>S</sub>	reflectance of Earth surface
r <sub>SAL</sub>	aluminium reflectance
r <sub>SC</sub>	collector reflectance
r <sub>SF</sub>	forest reflectance
r <sub>SG</sub>	ground reflectance
r <sub>SP</sub>	plastic reflectance
r <sub>SW</sub>	wheatland reflectance
r <sub>S1</sub> , r <sub>S2</sub>	local ground solar reflectances
S <sub>H</sub>	global surface heat power flux (W/m <sup>2</sup> )
S <sub>0</sub>	average solar flux on Earth (342 W/m <sup>2</sup> )
T <sub>A</sub>	Earth atmosphere temperature (K)
T <sub>S</sub>	Earth surface temperature (K)

## Greek symbols

σ	Stephan Boltzmann constant ( $5.67 \times 10^{-8}$ W/m <sup>2</sup> K <sup>4</sup> )
ε	hemispherical emissivity of the atmosphere

## References

- [1] Akbari H. Global cooling: increasing the world wide urban absorptances to offset CO<sub>2</sub>. Fifth annual California climate change conference, Sacramento, CA, [www.climatechange.ca.gov/events/2008\\_conference/presentations/2008-09-09/Hashem\\_Akbari.pdf](http://www.climatechange.ca.gov/events/2008_conference/presentations/2008-09-09/Hashem_Akbari.pdf); 9 September 2008.
- [2] Akbari H, Menon S, Rosenfeld A. Global cooling: increasing world-wide urban albedos to offset CO<sub>2</sub>. *Climatic Change* 2009;94:275–86.
- [3] Lenton TM, Vaughan NE. The radiative forcing potential of different climate geoengineering options. *Atmos Chem Phys Discuss* 2009;9:2559–608.
- [4] Nemet GF. Net radiative forcing from widespread deployment of photovoltaics. *Environ Sci Tech* 2009;43(60):2173–8.
- [5] Idealized greenhouse model, wikipedia, [http://en.wikipedia.org/wiki/Idealized\\_greenhouse\\_model](http://en.wikipedia.org/wiki/Idealized_greenhouse_model).
- [6] Knox RS. Physical aspects of the greenhouse effect and global warming. *Am J Phys* 1999;67(12):1227–37.
- [7] Keihl JT, Trenberth KE. Earth's annual global mean energy budget. *B Am Meteorol Soc* 1997;78:197–208.
- [8] IPCC. Climate change 2007: the physical science basis. Cambridge University Press, 2007.
- [9] Joos F, Bruno M, Fink R, Siegenthaler U, Stocker TF, LeQuere C, et al. An efficient and accurate representation of complex oceanic and biospheric models of anthropogenic carbon uptake. *Tellus B* 1996;48:397–417.
- [10] Price H. Parabolic trough technology overview. NREL, [http://www.ornl.gov/sci/engineering\\_science\\_technology/world/renewable/Trough%20Technology%20-%20Algeria2.pdf](http://www.ornl.gov/sci/engineering_science_technology/world/renewable/Trough%20Technology%20-%20Algeria2.pdf).
- [11] Schlaich J, Bergermann R, Schiel W, Weinreb G. Design of commercial solar tower system-utilization of solar induced convective flows for power generation. Proc. ISEC 2003, Hawaii, [http://www.sbp.de/de/fla/contact/download/The\\_Solar\\_Updraft.pdf](http://www.sbp.de/de/fla/contact/download/The_Solar_Updraft.pdf); March 2003.

- [12] Rafferty K. Geothermal power generation: a primer on low temperature, small scale application, <http://geoheat.oit.edu/pdf/powergen.pdf>.
- [13] Hansen FV. Albedos army research laboratory report AD-A268 255, <http://www.dtic.mil/cgi-bin/GetTRDoc?AD=ADA268255&Location=U2&doc=GetTRDoc.pdf>.
- [14] Albedos - wikipedia, [http://en.wikipedia.org/wiki/File:Albedo-e\\_hg.svg](http://en.wikipedia.org/wiki/File:Albedo-e_hg.svg).
- [15] Wu H, Fu Q, Giles R, Bartle J. Energy balance of Mallee biomass production in Western Australia. Bioenergy Australia 2005 – “Biomass for Energy, the Environment and Society”; Dec 2005. Melbourne.
- [16] Solar flagship program, [http://www.ret.gov.au/Department/Documents/CEI%20Fact%20Sheet%20\(13%20May%2009\).pdf](http://www.ret.gov.au/Department/Documents/CEI%20Fact%20Sheet%20(13%20May%2009).pdf).
- [17] Origin and carbon conscious agree large scale CPRS carbon forest sink deal, <http://www.originenergy.com.au/news/article/asxmedia-releases/1050>; July 16 2009.
- [18] Betts RA. Offset of the potential carbon sink from boreal forestation by decreases in surface albedo. *Nature* 2000;408:187–90.
- [19] Bala G, Caldeira K, Wickett M, Phillips TJ, Lobell DB, Delire C, et al. Combined climate and carbon-cycle effects of large-scale deforestation. *Proc Nat Acad Sci U S A* 2007;104(16):6550–5.
- [20] Betts RA, Falloon PD, Goldewijk KK, Ramankutty N. Biogeophysical effects of land use on climate: model simulations of radiative forcing and large scale temperature change. *Agr Forest Meteorol* 2007;142:216–33.
- [21] Stavins RN, Richards KR. The cost of U.S. forest-based carbon sequestration. Pew Centre on Global Climate Change, [http://www.pewclimate.org/docUploads/Sequest\\_Final.pdf](http://www.pewclimate.org/docUploads/Sequest_Final.pdf).
- [22] Midlands Landcare Education Website. <http://www.det.wa.gov.au/education/deo/midlands/Landcare/liyh/watersalwaysonthemove.htm>
- [23] BOM. [http://www.bom.gov.au/climate/map/evaporation/evap\\_ann.shtml](http://www.bom.gov.au/climate/map/evaporation/evap_ann.shtml)
- [24] Queensland Water Commission. [http://www.qwc.qld.gov.au/tiki-read\\_article.php?articleId=306](http://www.qwc.qld.gov.au/tiki-read_article.php?articleId=306)
- [25] Aqua Guardian Group Ltd, Melbourne. [www.aquaguardiangroup.com](http://www.aquaguardiangroup.com)
- [26] Queensland water commission desalination studies. Costing: p. C57, [http://www.qwc.qld.gov.au/myfiles/uploads/desal\\_studies\\_nov09/Appendix%20C\\_Costing%20\\_Final%20A.pdf](http://www.qwc.qld.gov.au/myfiles/uploads/desal_studies_nov09/Appendix%20C_Costing%20_Final%20A.pdf); Nov 2009.
- [27] Craig I, Green A, Scobie M, Schmidt E. Controlling evaporation loss from water storages, final report, <http://www.ncea.org.au/www/Evaporation%20Resources/Downloads/Contolling%20Evaporation%20Loss%20from%20Water%20Storages%20final%20report.pdf>; 2005.